Advances in Computer, Signals and Systems (2023)
Clausius Scientific Press, Canada

DOI: 10.23977/acss.2023.071109
ISSN 2371-8838 Vol. 7 Num. 11

Study on the optimization of ship survey line placement based on multibeam bathymetry

Yuankai Lin[1,#], Yuxin Chen[2,#], Yanzu Wu[2,#]

[1]School of Public Finance and Taxation, Zhejiang University of Finance & Economics, Hangzhou, 310018, China
[2]School of Economics, Zhejiang University of Finance & Economics, Hangzhou, 310018, China
[#]These authors contributed equally.

Keywords: Multibeam Bathymetry, Shortest Survey Line Placement, Single Objective Optimization model

Abstract: The multibeam bathymetry technology measures water depth strip by transmitting multiple beams through transducer, which is more efficient and accurate than the traditional bathymetry methods. In this paper, we focus on the measurement of the bathymetry of the sea area by multibeam sounding line. Firstly, we establish a two-dimensional discretization model to describe the relationship between the coverage width and the overlap rate of multibeam sounding. Secondly, we develop a three-dimensional mathematical model of the coverage width of the sounding vessel when facing the tilted seabed. Finally, by constructing the geometric model and single-objective optimization model, the shortest survey line planning scheme is given for the multibeam sounder while meeting the requirements of coverage and overlap rate. Through the construction of the above model, this paper draws the following conclusions: ① The distribution density of the survey line should be negatively correlated with the depth of the sea; ② Sailing along the isobath maximizes the width of the survey; ③ To achieve the shortest survey line, the direction of survey lines should always be parallel to the isobath.

1. Introduction

Multibeam bathymetry is an acoustic depth measurement technique based on the evolution of single-beam bathymetry[1]. It measures multiple bathymetric points on the seafloor within a section by transmitting and receiving several independent acoustic beams, thus obtaining a full-coverage bathymetric strip with a certain width. The emergence of single-beam bathymetry is an innovation in bathymetric surveying, which has the advantages of high efficiency and accuracy, continuous recording, and small impact on the environment, etc. However, it collects bathymetry point by point, and there is no bathymetric data between survey lines[2]. Compared to single-beam bathymetry, multibeam bathymetry technology is characterized by full coverage, high accuracy, high density, and high efficiency[3]. To ensure high-quality depth data, it incorporates additional sensor data to compensate for errors due to factors such as sound speed, vessel attitude, offset, and delay[4]. The results of multibeam sounding reflect the actual underwater conditions in detail, comprehensively and accurately, and have achieved good results in practical applications such as the deepwater

channel management project at the mouth of the Yangtze River and the dredging project of Zhanjiang Harbor channel [5,6].

However, in the process of multibeam bathymetry, the spacing between the survey lines affects the overlap rate between the bathymetric strips, which complicates the source of the side-generated data noise and affects the accuracy and efficiency of the bathymetry. The multibeam automatic filtering algorithm[7] and the addition of suitable portable measurement equipment [8]are the main focuses of scholars' research. The data are preprocessed by statistical filtering, and then the optimal reference surface is constructed based on the filtered topographic data, and the theoretical optimal depth value of each beam point is calculated. Narrow spacing and high overlap rate increase the bathymetric accuracy, but reduce the measurement efficiency; wide spacing and low overlap rate are highly efficient, but they reduce the resolution of seabed topography and may even cause leakage, which cannot guarantee the quality of measurement results. Therefore, it is the core issue to plan the survey line path rationally and adjust the spacing of survey lines according to the specific conditions. In this case, we can take both the coverage rate and efficiency of bathymetry into consideration, realizing the accurate measurement of the depth of the sea area. In addition, compared with the traditional multibeam bathymetry, the dual-probe multibeam system can acquire seabed topographic data quickly and efficiently, and its accuracy meets the relevant measurement standard[9,10]. However, the efficiency is reduced due to the unreasonable setting of spacing and overlap rate.

2. Modeling and Solving

2.1 Mathematical modeling for 2D planar multibeam bathymetry: coverage width and overlap rate between adjacent strips.

In multibeam bathymetric operation, the coverage width of a multibeam bathymetric strip W varies with the transducer opening angle θ and the water depth D. If the lines are parallel to each other and the seabed topography is flat, the overlap rate between neighboring strips is defined as $\eta = 1 - \frac{d}{w}$, where d is the spacing between two neighboring lines and W is the coverage width of the strip. If $\eta < 0$, a missed measurement is indicated. To ensure the convenience of measurement and data integrity, the overlap rate between neighboring strips should be 10%~20%. However, the real seabed topography varies greatly. If the average depth of water is used to design the line spacing, although the average overlap rate between the strips can meet the requirements, there will be omission of measurement in the shallow water depth (Fig 1), which affects the quality of the measurements; if the shallowest depth of water is used to design the line spacing, although the overlap rate of the shallowest water depth can meet the requirements, there will be excessive overlap in the deeper water depth (Fig 1) and this large data redundancy will affect the measurement efficiency.

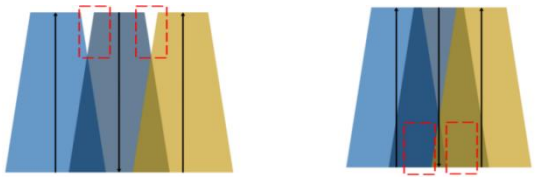

Figure 1: Schematic diagram of missed and overlapping areas

In this regard, before discussing the optimization of survey line laying, it is first necessary to solve the contradiction between the overlap rate and the coverage rate in the bathymetric work. To

construct the mathematical model of coverage width and overlap rate, the first step is to construct a right-angled coordinate system. Take the position of the right side of the ship as the origin and the straight line where the transverse axis of the ship is located as the x-axis to construct the right-angled coordinate system, as shown in Fig 2:

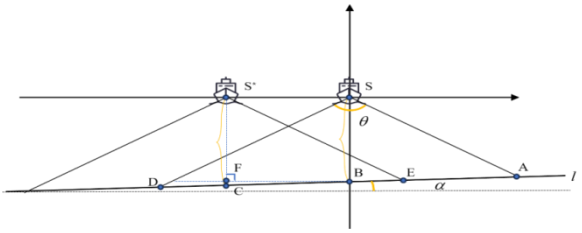

Figure 2: Schematic diagram of the right-angled coordinate system

Among them, S is the origin, S^* is the position of the neighboring vessel on the left. The distance between them is d. B、C are the intersection points between S、S^* perpendicular to the x axis and the slope surface l. The gradient of the slope l is α. The linear equation of the slope l is:

$$y = \tan(\alpha)x - y_B \tag{1}$$

A line parallel to the x-axis and intersecting S^*C at point F is drawn through point B. By the congruent angle theorem and the opposite angle theorem, it is known that:

$$\angle FBC = \alpha \tag{2}$$

According to the overlap ratio formula, it is known that $\eta = 1 - \frac{d}{W}$, where AD is the coverage width W. Solve for DE and AD separately:

$DE = BD + CE - CB$, where:

$$\begin{cases} BD = \dfrac{\sin(\theta/2)\times SB}{\sin(90^\circ - \alpha - \theta/2)} = \dfrac{\sin(\theta/2)\times(y_S - y_B)}{\sin(90^\circ - \alpha - \theta/2)} \\ CE = \dfrac{\sin(\theta/2)\times S^*C}{\sin(90^\circ - \alpha + \theta/2)} = \dfrac{\sin(\theta/2)\times(y_{S^*} - y_C)}{\sin(90^\circ - \alpha + \theta/2)} \\ BC = \dfrac{d}{\cos(\alpha)} = \dfrac{x_{S^*} - x_S}{\cos(\alpha)} \end{cases} \tag{3}$$

$AD = AB + BD$, where:

$$\begin{cases} AB = \dfrac{\sin(\theta/2)\times SB}{\sin(90^\circ + \alpha - \theta/2)} = \dfrac{\sin(\theta/2)\times(y_S - y_B)}{\sin(90^\circ + \alpha - \theta/2)} \\ BD = \dfrac{\sin(\theta/2)\times SB}{\sin(90^\circ - \alpha - \theta/2)} = \dfrac{\sin(\theta/2)\times(y_S - y_B)}{\sin(90^\circ - \alpha - \theta/2)} \end{cases} \tag{4}$$

In summary, the mathematical model of overlap rate and coverage width can be obtained as:

$$\eta = \frac{\frac{\sin(\theta/2)\times(y_S - y_B)}{\sin(90^\circ - \alpha - \theta/2)} + \frac{\sin(\theta/2)\times(y_{S*} - y_C)}{\sin(90^\circ - \alpha + \theta/2)} - \frac{x_{S*} - x_S}{\cos(\alpha)}}{W} \tag{5}$$

Among them:

$$W = \sin(\theta/2)\times(y_S - y_B)\left[\frac{1}{\sin(90^\circ + \alpha - \theta/2)} + \frac{1}{\sin(90^\circ - \alpha - \theta/2)}\right] \tag{6}$$

After establishing the mathematical model, this paper presets a simple two-dimensional planar seafloor scene. In this scene, the opening angle of the multibeam transducer θ is 120°, the slope α is 1.5°, the centroid is 70m from the seafloor, and the spacing of the two neighboring survey lines d is 200m. From this, we can get the coverage width and the overlap rate of the bathymetric vessel within the preset scene. The specific data are shown in Table 1.

Table 1: Coverage width and overlap rate data for preset scenarios

Distance of the line from the center/m	-800	-600	-400	-200	0	200	400	600	800
Sea depth/m	90.95	85.72	80.47	75.24	70	64.76	59.53	54.29	49.05
Coverage width/m	315.81	297.63	279.44	261.26	243.07	224.88	206.70	188.52	170.33
Overlap rate with previous line/%	--	35.70	31.15	26.74	21.26	14.89	7.41	0	0

2.2 Mathematical modeling of the coverage width of multibeam bathymetry in three dimension

After completing the two-dimensional model, we further discuss the establishment of a model in three-dimensional space. In this paper, two special planes are extracted from the three-dimensional space where the ship is located: the bathymetric cross-section and the plane formed by combining the normal vector of the horizontal plane and the direction of the survey line. In the two planes, the depth change model when sailing along the direction of the survey line and the slope change model caused by the change of heading are respectively established, so as to solve the coverage width model of the bathymetric vessel in the three-dimensional space.

Before modeling the depth variation of sailing along a survey line, it is necessary to place a hypothetical three-dimensional spatial rectangular sea area into the construction of a spatial Cartesian coordinate system. After building a spatial rectangular coordinate system, the longitudinal profile of a survey line can be obtained by combining any survey line direction with the normal vector of the horizontal plane, as shown in Fig 3.

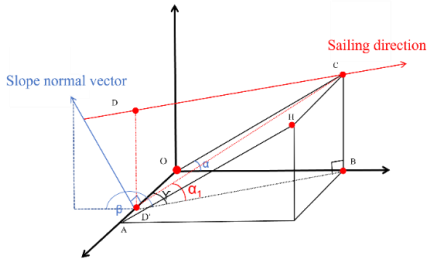

Figure 3: Longitudinal profile of the survey line in the spatial Cartesian coordinate system

Where β is the angle between the projection of the normal vector of the slope on the horizontal plane and the profile, i.e., the angle between the direction of the survey line and the projection of the normal direction of the submarine slope on the horizontal plane; α is the slope of the given slope; α_1 is the angle between the intersection line between the slope and the profile and the horizontal plane; γ is the angle between the profile and the x axis. The projection perpendicular to the xOy plane over the point D is made and intersects the x-axis at D'. So there exists:

$$\begin{cases} \gamma = \left| \beta - \dfrac{\pi}{2} \right| \\ \tan(\alpha) = \dfrac{BC}{OB} \\ \sin(\gamma) = \dfrac{OB}{BD'} \\ \tan(\alpha_1) = \dfrac{BC}{BD'} = \tan(\alpha) \times \sin(\gamma) \end{cases} \tag{7}$$

From this, it is possible to establish a function of the depth change when sailing in the direction of the survey line:

$$z = \tan(\alpha_1) \times \frac{y}{\sin(\gamma)} \tag{8}$$

$$Depth = L_z - z \tag{9}$$

where (x, y) denotes the coordinates of the vessel on the x and y axes in the spatial Cartesian coordinate system, z denotes the z axis coordinates of the vessel's projection on the slope, L_z represents the z axis coordinates of the sea level.

Then this paper starts to construct the slope change model caused by the change of heading, as shown in Fig. 4. Set $\overrightarrow{DC}$ as any line direction of the bathymetric vessel, DC as a line. Set $P_{(x,y,L_z)}$ as any point on the line, indicating that the bathymetric vessel is in any position on the line DC. $P_{(x,y,L_z)}EF$ is the bathymetric cross-section in that position and direction (shaped as the plane *SDA* in 2.1). EF is the intersection of the two planes of the bathymetric beam and the seabed slope surface. Project DC、EF onto the horizontal plane as $D'B$、$E'F'$. Project $P_{(x,y,L_z)}$ onto the sea floor slope and the horizontal plane as P' and P'' respectively as shown in Fig 4.

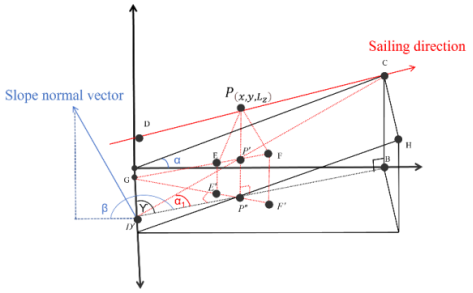

Figure 4: Bathymetric cross-section formed by projection

Connect the line $P'E$ and extend it to intersect the x axis at G . At this point, the degree of $\angle FGF'$ is α_2 , which is the slope of the bathymetric cross-section. This can be more clearly reflected in Fig 5 by stripping out the dihedral angle $G-P'P''-D'$.

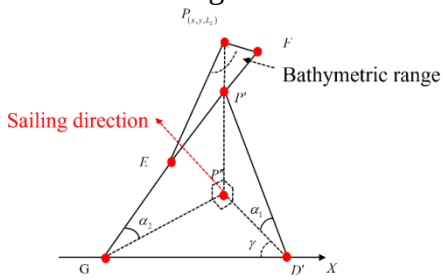

Figure 5: Bathymetric cross section with dihedral angle $G-P'P''-D'$ presented separately

It exists at this point:

$$\begin{cases} \tan(\gamma)=\dfrac{P''G}{P''D'} \\ \tan(\alpha_1)=\dfrac{P'P''}{PD'} \end{cases} \tag{10}$$

And because:

$$\tan(\alpha_2)=\frac{P'P''}{P''G} \tag{11}$$

So joining the two equations gives:

$$\tan(\alpha_2)=\frac{\tan(\alpha_1)}{\tan(\gamma)}=\frac{\tan(\alpha)\times\sin(\gamma)}{\tan(\gamma)}=\tan(\alpha)\times\cos\left(\left|\beta-\frac{\pi}{2}\right|\right) \tag{12}$$

This paper thus accomplishes the conversion of a single-direction slope α to the slope of a bathymetric cross-section α_2 in different directions and at different locations.

In summary, after constructing the depth change model for sailing along the direction of the survey line and the slope change model for different heading directions, this paper associates the solution model of the coverage width of the bathymetric vessel in 2.1 with the above model, and obtains the coverage width solution model as follows:

$$W=\frac{\sin(\theta/2)\times Depth}{\sin\left(90^{\circ}+\alpha_2-\theta/2\right)}+\frac{\sin(\theta/2)\times Depth}{\sin\left(90^{\circ}-\alpha_2-\theta/2\right)} \tag{13}$$

The above is the standard form of the mathematical model of the coverage width of multibeam bathymetry in three-dimensional space. But to facilitate the solution, a spatial right-angle coordinate system with the center sea area as the origin, the heading as the y-axis, the normal vector of the sea level over the origin as the z-axis, and the normal vector perpendicular to the plane xOy over the origin as the x-axis is re-established. This paper assumes that the seabed gradient of the three-dimensional sea area is 1.5 °, the depth of the sea at the center of the sea area is 120, and the opening angle of the multibeam transducer is 120 °. The depth of seawater at the center of the sea area is 120, and the opening angle of the multibeam transducer is 120 °. Then we can calculate the corresponding bathymetry coverage width of the ship at different positions and different directions

in the sea area. The results are shown in Table 2.

Table 2: Table of seafloor coverage widths for different positions and directions of the bathymetric vessel in the sea area

Coverage width/m		Distance between the center of the sea and the survey vessel /nautical mile							
		0	0.3	0.6	0.9	1.2	1, 5	1.8	2.1
Angle between survey directions/ °	0	415.69	466.09	516.49	566.89	617.29	667.69	718.09	768.48
	45	416.12	451.79	487.47	523.14	558.82	594.49	630.16	665.84
	90	416.55	416.55	416.55	416.55	416.55	416.55	416.55	416.55
	135	416.12	380.45	344.77	309.10	273.42	237.75	202.08	166.40
	180	415.69	365.29	314.89	264.50	214.10	163.70	113.30	62.90
	225	416.12	380.45	344.77	309.10	273.42	237.75	202.07	166.40
	270	416.55	416.55	416.55	416.55	416.55	416.55	416.55	416.55
	315	416.12	451.79	487.47	523.14	558.82	594.49	630.16	665.84

2.3 Optimization of the survey line layout of the shortest bathymetric vessel

After establishing the mathematical model between coverage width and overlap rate, and constructing a mathematical model for solving the bathymetric coverage width in three-dimensional space, this paper proceeds to construct the optimization model of the shortest bathymetric vessel survey line placement.

Before starting to construct the model, this paper firstly processes the given conditions and makes assumptions in advance to simplify the construction and calculation of the model, the specifics are as follows.

2.3.1 Modeling Preparation

(1) Gridding of maps

Considering that the coverage width of the measurements varies when the depth of sea floor is different, while the traveling direction of the ship may change, this paper grids the sea area and sets the grid edge length $patch\_size$ to be the projection of the sailing line segment on the y axis (i.e., one of the grids in the fig). The decision variables $startpoint_{ij}$ and deg_{ij} are introduced to represent the coordinates of the x axis and the walking angle at the j step of the i voyage, respectively. In particular, $j=0$ represents the state of the boat on the x axis when it is ready to depart. The route of the map after grid is shown in Fig 6.

(2) There is no difference between sailing from the middle and the edge

Due to the requirement of overlap rate, a certain distance should be maintained between routes during navigation. Taking the middle as the starting position needs to calculate to both sides, while taking the edge as the starting position only needs to consider one side, which is simpler. Since $startpoint_{ij}$ and deg_{ij} are decision variables in the iteration process, their randomized values and algorithmic iterations ensure no difference between sailing from the middle region and from the edge, this paper starts the iteration at the x-axis near the origin.

(3) The overlap rate should be between 10% and 20% wherever possible

In the process of actual bathymetry, it is necessary to balance between the overlap rate and the coverage width. This paper assumes that the overlap rate should be controlled between 10% and

20%. The shortest survey line placement is solved under this condition.

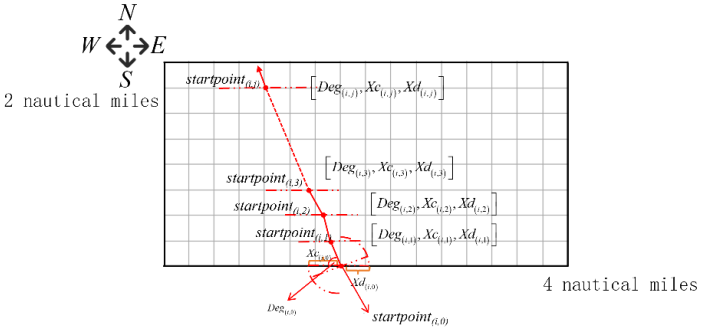

Figure 6: Gridded marching simulation

2.3.2 Gridded 2D planar iterative modeling

After making the above assumptions, this paper solves the shortest survey line placement by establishing a two-dimensional planar iterative model. First, the vector of the iterative boundary is set as $sidex$ and the initial iterative boundary vector is:

$$sidex = [0, 0, ...0], i \in 0, 1, 2... \tag{14}$$

From the above, the depth of the point, $depth_{ij}$, can be found from the position of $startpoint$. The widths of the point covered to the left and right can also be found, and their projections on the horizontal plane are denoted by Xc_{ij} and Xd_{ij}, respectively. As the model iterates, the state vector $sidex$ is updated to the projection of the current point with the farthest coverage to the right probe on the x axis, i.e.:

$$sidex[j] = X[D[ij]] + standpoint[ij] \tag{15}$$

In this model, the number of recorded walks $patch\_size$ is M. Since the sea is meshed into a large number of very small grids, the length of the y axis for each walk is fixed with coverage area and overlap requirements, so in this paper it can be approximated that the length of the walk on each $patch$ is the same. That is, to solve for the minimum value of the walk length, i.e., to solve for the minimum value of M.

The model should satisfy the following constraints:

Constraint I: Coverage of all areas.

Constraint II: Overlap rate of 10%-20%.

The overall mathematical model is described below:

$$\min M$$
$$s.t.\begin{cases} Xc_{ij}..startpoint_{ij}\ (i=1, j=0,1,...) \\ 0.1 \quad \dfrac{startpoint_{ij} - sidex[j]}{Xc_{ij}} \quad 0.2\ (i>1, j=0,1,...) \end{cases} \tag{16}$$

The model iteration is described as follows:

For the case of covering the y-axis region at $i=1$ and satisfying the overlap rate at $i>1$, when $j > length / patch\_size$, $i = i+1$. At this point, it has already reached the boundary and starts the

next round of detection.

The eventual exit mechanism is as follows:

When $startpoint[ij] < X[B] \& j = length / patchsize$, $X[B]$ is the length of the sea area. If the rightmost part of the sea is still not reached after j steps to the left, it means that all areas have been probed. From this, exit the loop and output the value of M. Find the minimum value of M for different decision variables $startpoint$ and deg by iteration.

This optimization model was translated into Python code and the Gurobi solver was called to solve for the shortest survey line placement in the 3D rectangular sea area. The final result is shown in Fig 7:

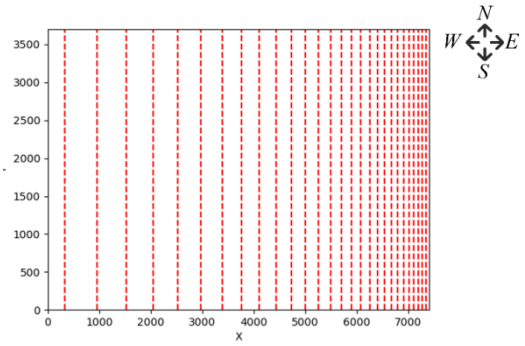

Figure 7: Map of shortest survey line placement

3. Conclusion

This paper reasonably uses the knowledge of spatial three-dimensional geometry to build a single-objective optimization model that solves the key indexes such as overlap rate and coverage width of multibeam bathymetry and proposes the shortest route scheme for the survey line layout. According to the output data of the above model in the hypothetical scenario, this paper comes up with the following suggestions on the survey line layout of multibeam bathymetry vessel.

From the calculation results of this paper, it is not difficult to find that with the increasing depth of seawater, the coverage width of the multibeam bathymetric instrument is increasing, and the overlap rate of two neighboring bathymetric strips is increasing. This paper concludes that when the depth is deeper, the survey line should be relatively sparse to improve the efficiency of bathymetry; when the depth is shallow, the survey line should be relatively dense to prevent leakage.

In the solution process of this paper, the center of the sea area is taken as the origin, so that the two sets of data with complementary angles in the direction of the survey line can be regarded as one survey line crossing the center of the sea area. After summing up the nodes on this whole survey line, it is found that the sum of the bathymetric coverage widths in the direction of the survey line sailing along the isobath (90, 270) is the largest, and the average bathymetric coverage width of each node is also the highest. Therefore, this paper concludes that if the bathymetric coverage of the survey line is to be as large as possible, the line should be laid along the isobath as much as possible. This conclusion is in line with the conclusions of existing studies[11] and also confirms the reliability and accuracy of the model of this topic.

From the final results of this paper, it is not difficult to find that the survey line becomes denser and sparser from west to east. Combined with the setting of "deeper in the west and shallower in the east", it is in line with the above conclusion that "the deeper the depth, the sparser the survey line placement, and the shallower the depth, the denser the survey line placement". It can be seen that the answer derived from solving the shortest line placement model is logically consistent with the

above conclusion and is reliable.

References

[1] Zhao, W., Zhuang, X., Wang, X., Zhou, L., 2022. Multi-beam Bathymetric measurement error analysis based on Integrated Navigation System, in: 2022 International Seminar on Computer Science and Engineering Technology (SCSET), IEEE, Indianapolis, IN, USA. pp. 174–178.

[2] Sun, Y.W., 2017 Underwater terrain measurement supported by GNSS high-precision dynamic height measurement mode. Shandong University of Science and Technology. shandong.

[3] Shi, X., 2023. Underwater Terrain Measurement Based on Unmanned Measurement Ship Multi-Beam Bathymeter, in: 2023 5th International Conference on Intelligent Control, Measurement and Signal Processing (ICMSP), IEEE, Chengdu, China. pp. 706–709.

[4] Grządziel, A. 2021. The importance of under - keel sound velocity sensor in measuring water depth with multibeam echosounder. Energies, 14 (17).

[5] Zhao Jianhu, Liu Jingnan. Current situation and development trend of multibeam bathymetry system. Hydrographic Surveying and Mapping, (3¬6), 2002.

[6] Ren Jianfu, Wei Zhongyang, Zhang Zhilin, etc. Application of EM2040C multibeam echosounder system in the quantitative monitoring of sea sand mining [J]. Bulletin of Surveying and Mapping , 2021(10): 136 - 140.

[7] Yan, Y., Yuan, L., Ran, L., Yin, H., Xiao, X., 2022. Multibeam Data Automatic Filtering Technology, in: 2022 3rd International Conference on Geology, Mapping and Remote Sensing (ICGMRS), IEEE, Zhoushan, China. pp. 224–228.

[8] Abubakar, A., Poerbandono, 2023. Effectiveness of vertical error budget model for portable multi-beam echo-sounder in shallow water bathymetric survey. IOP Conference Series: Earth and Environmental Science 1245, 012041.

[9] Guo, Q., Fu, C., Chen, Y., Zhang, Y., 2023. Application of multi-beam bathymetry system in shallow water area. Journal of Physics: Conference Series 2428, 012042.

[10] Grządziel, A., 2023. Method of Time Estimation for the Bathymetric Surveys Conducted with a Multi-Beam Echosounder System. Applied Sciences 13, 10139.

[11] Hong Demei, Zhang Xu, Ye Jian. Research on line laying method of multibeam system in Yangtze River channel surveying. China Water Transport. Waterway Science and Technology, (52¬55), 2017.